A Journal of the Gesellschaft Deutscher Chemiker

Angewandte International Edition Chemie

GDCh

www.angewandte.org

Accepted Article

Title: An expanded porphycene with high NIR absorptivity that stabilizes two different kinds of metal complexes

Authors: Gonzalo Anguera Pujadas, Won-Young Cha, Matthew Darren Moore, James Thomas Brewster II, Michael Ying Zhao, Vincent M Lynch, Dongho Kim, and Jonathan L. Sessler

To be cited as: *Angew. Chem. Int. Ed.* 10.1002/anie.201711197
Angew. Chem. 10.1002/ange.201711197

Link to VoR: http://dx.doi.org/10.1002/anie.201711197
http://dx.doi.org/10.1002/ange.201711197

WILEY-VCH

10.1002/anie.201711197

WILEY-VCH

COMMUNICATION

An expanded porphycene with high NIR absorptivity that stabilizes two different kinds of metal complexes

Gonzalo Anguera, Won-Young Cha, Matthew D. Moore, James T. Brewster II, Michael Y. Zhao, Vincent D. Lynch, Dongho Kim* and Jonathan L. Sessler*

Abstract: A new 26 π-electron expanded porphycene (**5**) has been prepared via McMurry coupling of 1,4-bis(3,4-diethyl-2-pyrryl)benzene dialdehyde. Expansion of the porphycene framework provides a ligand capable of stabilizing a bis-rhodium (**8**) and a ruthenium complex (**9**). These new porphycene derivatives absorb strongly in the NIR spectral region with appreciable absorptivity up to 1300 nm. On the basis of their ground and excited state spectroscopic features and structural parameters both the free-base system (**5**) and the bis-rhodium complex (**8**) are considered to be Hückel-type aromatic systems. This conclusion is supported by DFT calculations.

Porphycenes (**1**), reported in 1986 by Vogel and coworkers, were the first constitutional isomers of porphyrins.[1] They consist of two 2,2'-bipyrrole subunits linked by two ethylene-bridges.[2,3] The result is a planar, aromatic macrocycle formally known as [18]porphyrin (2.0.2.0). As true for porphyrins, porphycenes contain an 18 π-electron periphery. However, relative to porphyrins, porphycenes generally display stronger absorbance features in the far-red portion of the visible spectrum due to their lower symmetry.[4] Porphycenes have been explored for a range of applications, including as photosensitizers for photodynamic therapy[5–7] and as ligands for catalysis.[8–10] Whereas expanded versions of porphyrins have been widely studied,[11–13] expanded porphycenes are all but unknown. Examples include bronzaphyrin (**2**)[14] and an acetylene-cumulene porphycene derivative (**3**).[15,16] Both **2** and **3** display red-shifted absorption features compared to **1**, reflecting an increase in the electronic pathway, from 18 to 26 π-electrons. The annulated *meso*-dibenzoporphycene derivative (**4**) also displays a red-shifted NIR infrared absorption maximum.[17] However, neither **2** or **3** (nor **4** or any other porphycene derivative of which we are aware) has been reported as being effective in stabilizing a bis-metal complex. We thus sought to prepare an expanded porphycene derivative that would both display strong NIR absorption features and permit the coordination of more than one metal center. As detailed below, the 26 π-electron phenylene-bridged expanded porphycene (**5**) fulfills both these design objectives. We have also found that this system can be used to produce a sandwich-type organometallic complex wherein the organic framework has undergone ring contraction.

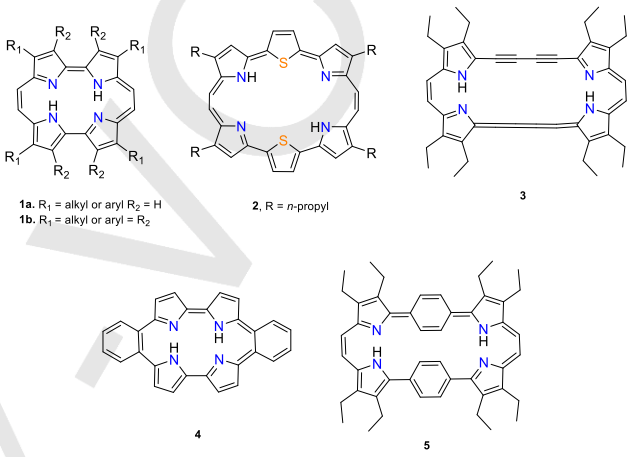

Scheme 1. Porphycene **1a**, ethioporphycene **1b**, bronzaphyrin **2**, acetylene – cumulene porphycene **3**, dibenzoporphycene **4**, and expanded porphycene **5**.

In an effort to obtain a porphycene derivative with a larger central cavity and with an extended π-electron periphery, we sought to incorporate a benzene spacer between the two formal halves of the porphycene core. With such considerations in mind, the dipyrrolylbenzene precursor **6** reported by Setsune et al.[18,19] was subject to formylation to produce **7** in 93% yield. An ensuing McMurry reaction and oxidation with 2,3-dichloro-5,6-dicyano-*p*-benzoquinone (DDQ) gave the extended porphycene **5** in 14% yield (Schemes 1 & 2). The relatively low solubility of the product allowed for simple recrystallization from CH_2Cl_2:hexanes. Solutions of **5** in chlorinated solvents are dark-red; however, a green metallic luster is seen in the solid state. An analysis of the ^{1}H-NMR spectrum ($CDCl_3$) revealed signals characteristic of an aromatic Hückel type macrocycle.[20] For instance, ethylene signals are seen at 9.16 ppm, along with benzene C*H* proton resonances at 4.40 ppm (8H) (cf. Fig. S5). The presence of only one such averaged C*H* signal is consistent with a conformationally mobile system, wherein the two benzene subunits undergoing fast rotation on the NMR time scale. A correlation spectroscopy (COSY) spectral study supports the broad signal at 3.90 – 3.76 ppm (8H) being assigned to the -CH_2CH_3 protons (cf. Fig. S6).

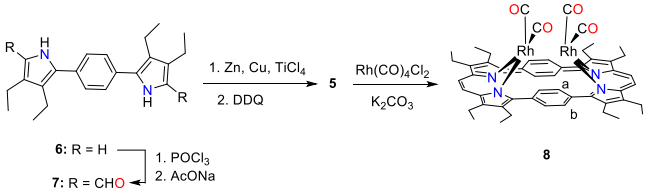

Scheme 2: Synthesis of expanded porphycene **5** and complex **8**.

[a] Dr. G. Anguera, M. D. Moore, J. T. Brewster, M. Y. Zhao, Dr. V. D. Lynch, Prof. J. L. Sessler.
Department of Chemistry, The University of Texas at Austin, 105 East 24th Street, Stop A5300, Austin, Texas, 78712 – 1224, United States
E-mail: sessler@cm.utexas.edu
[b] J. T. Brewster and Prof. J. L. Sessler.
Center for Supramolecular Chemistry and Catalysis, Shanghai University, Shanghai 200444, China
[c] Dr. W.-Y. Cha, Prof. D. Kim
Spectroscopy Laboratory for Functional π-Electronic Systems and Department of Chemistry, Yonsei University, Seoul 03722, Korea.

Supporting information and the ORCID identification number(s) for the author(s) of this article can be found under:

Crystal data may be obtained from the Cambridge Crystallographic Centre CCDC numbers 1580306, 1580307 and 1581856

10.1002/anie.201711197

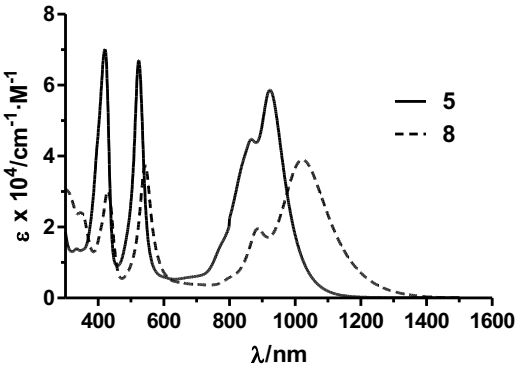

Figure 1. Steady-state absorption spectra of the expanded porphycene **5** (solid line) and its bis-rhodium complex **8** (dashed line) in $CHCl_3$.

An analysis of its UV-vis-NIR absorption spectrum provides further support for the Hückel type aromaticity proposed for compound **5** (Figure 1). In particular, in chloroform solution two Soret-like bands at λ_{max} (ε) = 420 nm (7.0 x 10^4 $M^{-1}\cdot cm^{-1}$) and 523 nm (6.7 x 10^4 $M^{-1}\cdot cm^{-1}$), as well as a broad Q-band at 923 nm (5.9 x 10^4 $M^{-1}\cdot cm^{-1}$), are seen. These bands are red-shifted relative to those of porphycene **1b** (cf. Table S1). Compared with other porphycene derivatives, **5** displays higher absorption maxima and larger extinction coefficients, and a low energy Q-band that extends into the NIR spectral region (cf. Table S1). The extended porphycene **4** also absorbs into the NIR (**4**, λ_{max} = 1047 nm). However, the extinction coefficients of its Q-bands are ≤ 5 x 10^3 $M^{-1}\cdot cm^{-1}$ (vs. **5**, λ_{max} = 923 nm, 5.9 x 10^4 $M^{-1}\cdot cm^{-1}$). Compound **2** displays higher extinction coefficients (i.e., up to 1 x 10^5 $M^{-1}\cdot cm^{-1}$). However, it absorbs at higher energies than either **4** or **5** (i.e., for **2**, λ_{max} = 889 nm). Compound **5** does not exhibit fluorescence in the NIR region in $CHCl_3$. However, in paraffin oil, a highly viscous medium that may obstruct rotation of the bridging phenyl groups, **5** gives rise to an observable fluorescence (cf. Fig. S21). A small Stokes shift of 710 cm^{-1} is observed; this is taken as evidence that the excited state is relatively rigid.

In an effort to obtain insight into the intense NIR absorption bands of compound **5**, we performed molecular optimization and TDDFT calculations at the B3LYP/6-31G(d,p) level. The energy minimized molecular structure of **5** was found to be very similar to the X-ray crystal structure. The simulated UV-vis spectrum of **5** was also found to coincide with the steady-state absorption spectrum. On the basis of these calculations, the electronic vertical transitions corresponding to the two Soret-like bands and two Q-type bands observed in the steady-state absorption spectrum of **5** mainly involve HOMO-1, HOMO, LUMO and LUMO+1. These orbitals are all characterized by delocalized π-electron densities through 26 π-electronic circuits (cf. Fig. S29). Two different electronic vertical transitions, in the visible and NIR regions, induce splitting in the Soret-like bands and Q-bands, respectively (cf. Fig. S29).

Nucleus independent chemical shift (NICS) calculations[21] were carried out in an effort to gain insight into the magnetic shielding effects present in compound **5** (cf. Fig. S30). The negative nature of these values (e.g., -15.11 ppm at the center of the ring) is consistent with the proposed aromatic character. An anisotropy of the current (induced) density (ACID) plot (Figure 2),[22] which directly displays the magnitude and direction of the induced ring current under an external magnetic field applied to the molecular plane, was also constructed. The π-conjugation pathway of **5** has a substantial electron density in the planar molecular framework, and a clear and definite clockwise current. In addition, a harmonic oscillator model of aromaticity (HOMA)[23] analysis of the π-conjugation pathways using the energy minimized molecular structure and the X-ray diffraction data for **5** (*vide infra*) was carried out. The resulting HOMA values were calculated to be 0.73 and 0.79 for these two inputs (cf. Fig. S31), respectively. The large HOMA value for **5** and its planar structure are again most easily rationalized in terms of this expanded porphycene having [4n+2] Hückel aromatic character.

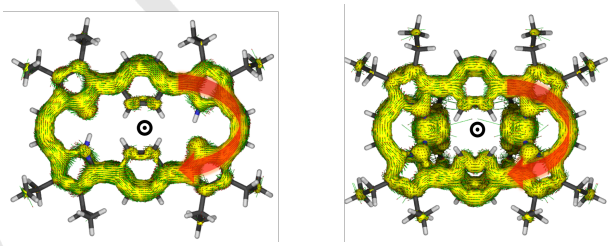

Figure 2. ACID plot of **5** (left) and **8** (right). Current density vectors indicate clockwise current, when viewed from the front and facing the direction of the external magnetic field vector (clockwise currents are diatropic). Isosurface value is 0.05.

Single crystals suitable for X-ray diffraction analysis were grown via slow evaporation of an initial CH_2Cl_2/hexanes (1:1, v/v) solution. As can be seen from inspection of Figure 3, **5** shows a largely planar macrocyclic ring system. Only the benzene subunits are appreciably tilted out of the plane, presumably due to CH --- HC steric interactions. The torsion angles between the pyrroles and the phenylene subunits range from 21.03 to 15.04°. Further analysis of the crystal structure reveals the presence of a cavity that is noticeably larger than that present in porphycene **1b**,[24] for which the N1-N2 (= N3-N4) distance is 2.732 and the N1-N3 (= N2-N4) separation is 2.799 Å. In contrast, in **5** the corresponding values are 7.06 Å for N1-N2 (= N3-N4) and 2.768 Å for N1-N3 (= N2-N4). The four nitrogen rectangle present in **5** defines an area of almost 20 $Å^2$, while the internal are of typical porphycenes (**1b**) is closer to 7 $Å^2$.[1] The large cavity in **5** led us to explore whether it could support the complexation of more than one metal center.

In order to study the reactivity of **5**, metal insertion studies were carried out with salts of palladium, platinum, copper, nickel and zinc; however, in no cases could a readily characterized product obtained. Generally, starting material was recovered. Likely the presence of the benzene subunit in the structure prevents the complexation of these metal cations. Several carbonyl reagents of rhodium and ruthenium have been used in the literature for the preparation of bidentate complexes of pyrroles derivatives, such as $Rh_2(CO)_4Cl_2$ and $Ru_2(CO)_6Cl_4$. For instance, Setsune and coworkers prepared multinuclear rhodium

10.1002/anie.201711197

complexes of different expanded porphyrins by simply stirring the rhodium precursor in degassed dichloromethane in the presence of K_2CO_3 and the ligand.[18] The same methodology was applied to compound **5** (Scheme 2) and, after silica gel column purification, the bis-rhodium complex (**8**) was obtained in 50% yield. In stark contrast with **5**, compound **8** is highly soluble in chlorinated solvents. This is attributed to the elimination of intermolecular π-π interactions.

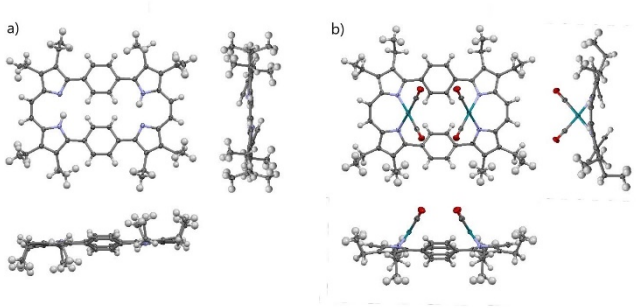

Figure 3. X-ray crystal structures of **5** (a) and **8** (b) as viewed from the top, side and bottom, respectively. Displacement ellipsoids are scaled to the 50% probability level.

^{1}H-NMR spectroscopic analysis of **8** reveals notable differences with the free base. To resolve all expected proton signals from **8**, a variable temperature ^{1}H-NMR spectral study was carried out using d_8-toluene as the solvent (cf. Fig. S10). Below -20 °C, two signals can be observed at 9.98 ppm (b, Scheme 1, 4H) and -0.45 ppm (a, Scheme 1, 4H) that are not seen at room temperature, both shifts being indicative of [4n + 2] π-electron Hückel-type aromaticity. The best resolved ^{1}H-NMR spectrum is seen at -40 °C (cf. Fig. S9). These resonances are assigned to the inner- and outward pointing CH protons on the bridging phenylene subunits, respectively. In contrast, in the ^{1}H-NMR spectrum of **5**, the C*H*-benzene signal is not split even at low temperature and appears as a time averaged signal at 4.40 ppm (8H).

Further support for the proposed Hückel aromaticity of complex **8** came from an analysis of its UV-vis spectrum (Figure 1). Relative to the free-base **5**, the larger Q-type band of **8** is characterized by a ca. 90 nm bathochromic shift (λ_{max} (**5**) = 923 nm; λ_{max} (**8**) = 1014 nm). Even more than in the case of **5**, the absorption features of **8** tail into the NIR. The complex itself is light red as a dilute chloroform solution. However, the maximum molar absorptivity of **8** ($\varepsilon = 3.9 \times 10^4$ $M^{-1}\cdot cm^{-1}$) is lower than that of **5** (see above). In noted contrast to what is true for most porphyrin derivatives, complex **8** is characterized by a higher extinction coefficient for the Q-band than for the Soret band. Compound **8** does not exhibit appreciable luminescence.

Single crystals suitable for X-ray diffraction analysis were grown via the slow diffusion of methanol into a chloroform solution of **8**. From an inspection of Figure 3b it can be observed that both rhodium centers are complexed on the same face of the macrocycle. The torsion angle about C3-C4-C5-C6 is 161.41° (cf. Table S14). The presence of the two rhodium di-carbonyl groups on the same side of the macrocycle provides support for the ^{1}H-NMR spectral assignment made for the CH-phenylene signals, namely that free rotation of the phenylene bridges will be blocked and that a greater number of CH signals should be observed in the ^{1}H-NMR spectrum of **8** than **5**.

For complex **8,** structural optimization and TDDFT calculations were carried out at the B3LYP/LANL2DZp level to account for the presence of the rhodium atoms. The energy minimized molecular structure of **8** is similar to the solid-state structure and the simulated absorption spectrum matches well with the experimental spectrum as recorded in chloroform (cf. Fig. S32). As true for compound **5**, complex **8** is characterized by a negative NICS value (-8.73 ppm) at the center of the complex (cf. Fig. S33). An ACID plot (Figure 2) of **8** revealed a clear and definite clockwise current within the [26]hexaphyrin-like framework. A 0.66 HOMA value for **8**, obtained by analysis of the X-ray diffraction data, is consistent with the proposed Hückel aromatic character (cf. Fig. S34).

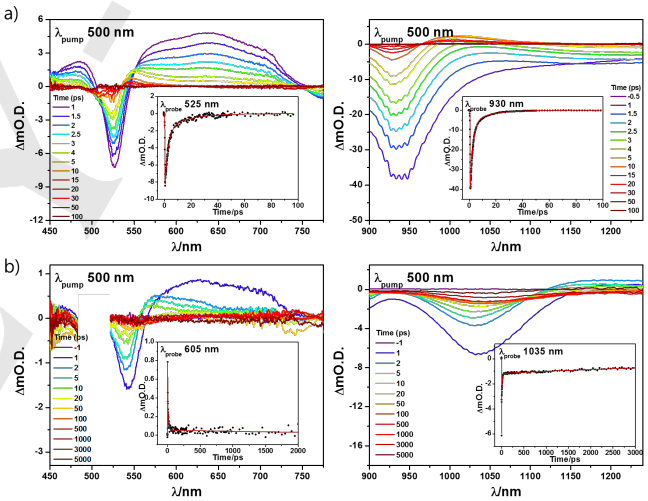

Figure 4. TA spectra of the (left) visible and (right) NIR spectral regions and decay profiles (insets) of **5** (a) and **8** (b) in toluene.

To understand in greater detail the optical features of **5** and **8**, their excited-state dynamics were probed using femtosecond transient absorption (TA) spectroscopy (Figure 4). Both **5** and **8** exhibit prominent excited-state absorption (ESA) and ground-state bleaching (GSB) signals that correspond to their steady-state absorption features. Compound **5**, in particular, gives rise to intense GSB signals and a relatively weak ESA spectrum in the NIR region. Such observations are typical of what is seen in the case of aromatic expanded porphyrins.[25] As expected given its non-fluorescent nature, the excited-state lifetime of **5** was estimated to be 1.4 ps in toluene a value that is shortened to 1.0 ps in the case of **8**. Presumably, this reduced lifetime is the result of efficient intersystem crossing due to the heavy atom effect of the coordinated rhodium metal cations. The observation of long residual TA signals (up to 3 ns) is consistent with the population of an excited-state triplet. Taken in concert, these spectroscopic

features provide further evidence for the [4n+2] Hückel-type aromaticity proposed for **5** and **8**.

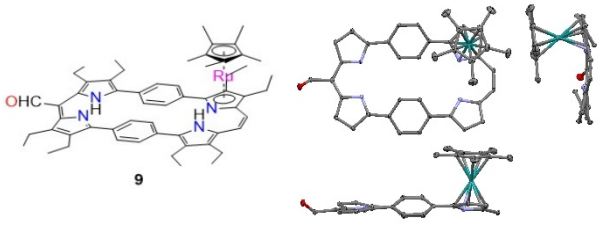

Figure 5. X-ray crystal structure of **9** as viewed from the top, side and bottom, respectively. Displacement ellipsoids are scaled to the 50% probability level. Substituents and hydrogens have been omitted for clarity

In a further test of **5** as a ligand, it was treated with $[Ru(Cp^*)(CH_3CN)_3][PF_6]$. In analogy to prior work,[26] this was expected to afford a sandwich-type organometallic complex. After purification, a blue-green compound with high solubility in organic solvents was obtained. In stark contrast with **5**, the ^{1}H-NMR spectrum revealed signals consistent with a non-aromatic species (cf. Fig. S12). Furthermore, the UV-vis spectrum of this product was characterized by a λ_{max} (ε) at 605 nm (1.5×10^4 $M^{-1} \cdot cm^{-1}$) (cf. Fig. S23), while HRMS analysis proved consistent with a complex with the formula $C_{58}H_{68}N_4ORu$ (cf. Fig. S19). A single crystal X-ray diffraction study revealed a structure wherein the expanded porphycene core had undergone rearrangement to provide a contracted species with a formylated single carbon bridge, **9** (Figure 5). To our knowledge such a conversion is without precedent in the porphycene literature and serves to highlight another unusual feature of the present expanded porphycene.

In conclusion, a new expanded porphycene **5** containing a formal 26 π-electron periphery has been prepared via the McMurry coupling of precursor **7** in 14% yield. Treatment of **5** with $Rh_2(CO)_4Cl_2$ gives rise to the corresponding bis-rhodium complex, **8**. Both compounds display Hückel aromatic character, as inferred from ^{1}H-NMR, UV-vis and DFT calculations. The UV-vis spectrum of **5** and **8** is characterized by a NIR infrared Q-band with a λ_{max} at 923 nm and λ_{max} at 1014 nm, respectively, in $CHCl_3$. The present work serves to confirm that it is possible to create expanded porphycenes that both show good NIR absorbing spectral features and which act as ditopic ligands capable of supporting complexes containing more than one metal center. Furthermore, upon treatment with $[Ru(Cp^*)(CH_3CN)_3][PF_6]$ the free-base system **5** was found to produce a non-aromatic, one carbon contracted ruthenium complex **9**. We thus believe that larger analogues of porphycene may be of interest in stabilizing unusual metal complexes and generating novel organic frameworks that lack analogy in the well-studied parent system.

Acknowledgements

G.A. thanks Fundación Ramón Areces (Madrid, Spain) for a postdoctoral fellowship. This work was supported by the National Science Foundation (grant CHE-1402004 to J.L.S.) and the Robert A. Welch Foundation (F-0018 to J.L.S.). The work at Yonsei University was supported by the National Research Foundation of Korea (NRF) grant funded by the Korea government (MEST) (2016R1E1A1A01943379). J.T.B would like to thank the NSF for an EAPSI fellowship.

Conflict of Interest

The authors declare no conflict of interest

Keywords: porphycene • macrocycles • NIR • rhodium • McMurry

[1] E. Vogel, M. Köcher, H. Schmickler, J. Lex, *Angew. Chemie Int. Ed.* **1986**, *25*, 257–259.
[2] D. Sánchez-García, J. L. Sessler, *Chem. Soc. Rev.* **2008**, *37*, 215–232.
[3] G. Anguera, D. Sánchez-García, *Chem. Rev.* **2017**, *117*, 2481–2516.
[4] J. Waluk, *Chem. Rev.* **2017**, *117*, 2447–2480.
[5] R. Dosselli, C. Tampieri, R. Ruiz-González, S. De Munari, X. Ragàs, D. Sánchez-García, M. Agut, S. Nonell, E. Reddi, M. Gobbo, *J. Med. Chem.* **2013**, *56*, 1052–1063.
[6] J. C. Stockert, M. Cañete, A. Juarranz, A. Villanueva, R. W. Horobin, J. I. Borrell, J. Teixidó, S. Nonell, *Curr. Med. Chem.* **2007**, *14*, 997–1026.
[7] X. Ragàs, D. Sánchez-García, R. Ruiz-González, T. Dai, M. Agut, M. R. Hamblin, S. Nonell, *J. Med. Chem.* **2010**, *53*, 7796–7803.
[8] R. Bernstein, C. S. Foote, *J. Phys. Chem. A* **1999**, *103*, 7244–7247.
[9] T. Matsuo, D. Murata, Y. Hisaeda, H. Hori, T. Hayashi, *J. Am. Chem. Soc.* **2007**, *129*, 12906–12907.
[10] A. Berlicka, B. König, *Photochem. Photobiol. Sci.* **2010**, *9*, 1359.
[11] J. L. Sessler, D. Seidel, *Angew. Chemie Int. Ed.* **2003**, *42*, 5134–5175.
[12] T. Sarma, P. K. Panda, *Chem. Rev.* **2017**, *117*, 2785–2838.
[13] J. Setsune, *Chem. Rev.* **2017**, *117*, 3044–3101.
[14] M. R. Johnson, D. C. Miller, K. Bush, J. J. Becker, J. A. Ibers, *J. Org. Chem.* **1992**, *57*, 4414–4417.
[15] A. Rana, S. Lee, D. Kim, P. K. Panda, *Chem. - A Eur. J.* **2015**, *21*, 12129–12135.
[16] C. Bernard, J. P. Gisselbrecht, M. Gross, N. Jux, E. Vogel, *J. Electroanal. Chem.* **1995**, *381*, 159–166.
[17] K. Oohora, A. Ogawa, T. Fukuda, A. Onoda, J. Hasegawa, T. Hayashi, *Angew. Chemie Int. Ed.* **2015**, *127*, 6325–6328.
[18] J. Setsune, M. Toda, T. Yoshida, *Chem. Commun.* **2008**, 1425–7.
[19] J. Setsune, M. Toda, T. Yoshida, K. Imamura, K. Watanabe, *Chem. - A Eur. J.* **2015**, *21*, 12715–12727.
[20] S. Saito, A. Osuka, *Angew. Chemie Int. Ed.* **2011**, *50*, 4342–4373.
[21] P. V. R. Schleyer, C. Maerker, A. Dransfeld, H. Jiao, N. J.

10.1002/anie.201711197

R. Van Eikema Hommes, *J. Am. Chem. Soc.* **1996**, *118*, 6317–6318.

[22] D. Geuenich, K. Hess, F. Köhler, R. Herges, *Chem. Rev.* **2005**, *105*, 3758–3772.

[23] T. M. Krygowski, M. Cyrański, *Tetrahedron* **1996**, *52*, 1713–1722.

[24] E. Vogel, P. Koch, X.-L. Hou, J. Lex, M. Lausmann, M. Kisters, M. A. Aukauloo, P. Richard, R. Guilard, *Angew. Chemie Int. Ed.* **1993**, *32*, 1600–1604.

[25] Y. M. Sung, J. Oh, W.-Y. Cha, W. Kim, J. M. Lim, M.-C. Yoon, D. Kim, *Chem. Rev.* **2017**, *117*, 2257–2312.

[26] L. Cuesta, E. Karnas, V. M. Lynch, P. Chen, J. Shen, K. M. Kadish, K. Ohkubo, S. Fukuzumi, J. L. Sessler, *J. Am. Chem. Soc.* **2009**, *131*, 13538–13547.

10.1002/anie.201711197

WILEY-VCH

Entry for the Table of Contents (Please choose one layout)

Layout 1:

COMMUNICATION

A new expanded porphycene prepared from the McMurry reaction of 1,4-bis(3,4-diethyl-2-pyrryl)benzene dialdehyde has been prepared. This extended tetrapyrrolic macrocycle displays Hückel type aromaticity (4n + 2 π electrons, n = 6), as inferred from NMR and UV-vis spectroscopies, as well as CV, DFT calculations, and TA studies. It was found to support the formation of both an aromatic bis-rhodium and non-aromatic, ring contracted "sandwich-type" mono-ruthenium complex.

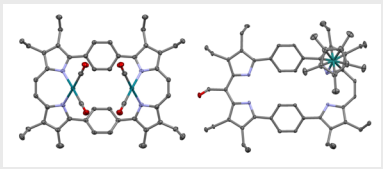

*Author(s), Corresponding Author(s)**

Page No. – Page No.

Title